IOP Publishing Journal of Physics A: Mathematical and Theoretical
J. Phys. A: Math. Theor. **53** (2020) 185701 (17pp) https://doi.org/10.1088/1751-8121/ab7e52

Dynamics of the nonholonomic Suslov problem under periodic control: unbounded speedup and strange attractors

Ivan A Bizyaev[1] and Ivan S Mamaev[2,3,4]

[1] Udmurt State University, ul. Universitetskaya 1, Izhevsk, 426034 Russia
[2] Izhevsk State Technical University, ul. Studencheskaya 7, Izhevsk, 426069 Russia
[3] Institute of Mathematics and Mechanics of the Ural Branch of RAS, ul. S. Kovalevskoi 16, Ekaterinburg, 620990 Russia

E-mail: bizaev_90@mail.ru and mamaev@rcd.ru

Received 30 November 2019, revised 11 February 2020
Accepted for publication 10 March 2020
Published 10 April 2020

Abstract

This paper is concerned with the study of a nonholonomic system with parametric excitation, the Suslov problem with variable gyrostatic momentum. A detailed analysis is made of the problem of the existence of regimes with unbounded growth of energy (an analog of Fermi's acceleration). The existence of trajectories is shown for which the angular velocity of the rigid body increases indefinitely and has the asymptotics $t^{\frac{1}{2}}$.

Keywords: nonholonomic mechanics, Fermi's acceleration, Suslov problem, unbounded speedup, strange attractor, rotor

(Some figures may appear in colour only in the online journal)

Introduction

In recent years, nonholonomic systems have attracted the attention of many researchers both from a purely theoretical point of view [1–3] and from the viewpoint of applications [4–6]. Much of this interest stems from the fact that these systems can exhibit a wide spectrum of dynamical effects inherent in conservative and dissipative systems. We illustrate this property of multivariance of the dynamical behavior of nonholonomic systems by a concrete mechanical problem, the *Suslov system with parametric excitation*.

We recall that a rigid body with a fixed point is said to be the Suslov system if it moves subject to the following nonholonomic constraint: the projection of the angular velocity onto

[4] Author to whom any correspondence should be addressed.

the body-fixed axis is zero. This constraint was proposed by G K Suslov in [7, p 593], and its correct realization was proposed by V Vagner [8]. The rigid body subject to this constraint executes inertial motion inside a fixed spherical shell to which it is connected by means of two wheels with sharp edges.

The Suslov system reduces to investigating a two-dimensional (integrable) reduced system governing the evolution of the angular velocity of the body [9, 10]. The motion of a rigid body in a fixed coordinate system is discussed in detail in [11].

There are a few well-known generalizations of the Suslov problem. For example, in [12, 13] the external spherical shell is assumed to be free (*nonholonomic hinge*) or rolling without slipping on a plane [14]. In [15, 16], the dynamics of the Suslov problem in a gravitational field is considered. It is shown that in this case the reduced system can exhibit a strange attractor and the effect of reversal. The authors of [17] address a problem in which the projection of the angular velocity of the rigid body onto the fixed axis takes a constant value (an inhomogeneous Suslov constraint). Various multidimensional generalizations of the Suslov problem are discussed in [18, 19]. Problems concerning the nonintegrability of various generalizations of the Suslov problem are dealt with in [1, 20, 21].

This paper continues a series of studies [14, 22–25] on the dynamics of nonholonomic systems with mass distribution periodically depending on time (parametric excitation). We note that the recent surge of interest in these problems is due to the importance of nonholonomic systems for mobile robotics applications. The problem of possible acceleration of a mobile system by means of a mechanism undergoing small regular oscillations is of great interest from this point of view.

We note that the Suslov system is closely related to another nonholonomic system, the *Chaplygin sleigh*. The latter can be obtained from the Suslov system using the procedure of retraction of the group SO(3) in SE(2) [26]. Earlier, two modifications of the Chaplygin sleigh [27] with parametric excitation were considered: *variable gyrostatic momentum* [23] and *a material point which executes periodic oscillations* [14, 22, 24]. In both cases, one observes an unbounded speedup in which the angular velocity of the sleigh tends to zero and the translational velocity increases indefinitely as $t^{\frac{1}{3}}$. Note that such a speedup $\left(\sim t^{\frac{1}{3}}\right)$ differs greatly from speedup under the action of an external periodic force with nonzero average value, for which the velocity increases in proportion to time t. The influence of the viscous friction force on the dynamics of the Chaplygin sleigh with parametric excitation is discussed in [23, 28, 29].

In this paper, we consider the Suslov system with parametric excitation. We assume that the moving rigid body has two rotors placed inside, which rotate with a given angular velocity depending periodically on time. This problem reduces to investigating a nonautonomous two-dimensional reduced system governing the evolution of the angular velocity of the rigid body.

In contrast to the Chaplygin sleigh with gyrostatic momentum, the reduced system considered in this work exhibits, depending on the functions defining the gyrostatic momentum $\Lambda(t)$ and $K(t)$, more diversity in its dynamical behavior:

(a) *Regular behavior*, when the problem reduces to investigating a vector field on a torus. The torus can display limit cycles and quasi-periodic trajectories (see section 2).

(b) *Speedup*, when for all initial conditions one component of the angular velocity increases indefinitely as $t^{\frac{1}{2}}$ or $t^{\frac{1}{3}}$ (see sections 3 and 4).

(c) *Chaotic dynamics*: the system has a strange attractor. An intermediate situation can also take place in which, depending on initial conditions, one part of trajectories is unbounded and the other part belongs to a strange attractor (i.e., it slows down) (see sections 4 and 5).

Of interest for further research is the question of the possibility of speedup in nonholonomic robots with a more complex control mechanism, see, e.g., references [4, 5, 30, 31], in which the control of a spherical robot is discussed. The conditions of speedup in such systems have yet to be studied.

1. Equations of motion

Consider the motion of a multicomponent mechanical system (see figure 1), which includes:

(a) *A fixed spherical shell*;
(b) *A rigid body* connected to the shell by means of two wheels with sharp edges in such a way that the rigid body cannot rotate about the fixed vector $\boldsymbol{e}$:

$$(\boldsymbol{\omega}, \boldsymbol{e}) = 0, \tag{1}$$

where $\boldsymbol{\omega}$ is the angular velocity of the body.
(c) *Two axisymmetric rotors* whose axis of rotation is rigidly attached to the rigid body and whose angular velocities $\Omega_1(t)$ and $\Omega_2(t)$ change with time.

As can be seen, the point O of the rigid body, which is at the geometric center of the shell, remains fixed. In this paper, we also assume that the common center of mass of the rigid body and the rotors coincides with the fixed point O. As a result, *the rigid body executes inertial motion*, since the force of gravity has no effect on its motion.

To describe the motion of the rigid body, we choose two coordinate systems:

(a) An *inertial* (fixed) coordinate system $OXYZ$ with origin at the fixed point O;
(b) A *noninertial* (moving) coordinate system $Ox_1x_2x_3$ chosen in such a way that $Ox_3 \| \boldsymbol{e}$.

The configuration space of this system coincides with the rotation group $\mathcal{N} = \mathrm{SO}(3)$; its elements are rotation matrices $\mathbf{Q}$, and each of these matrices specifies the orientation of the body in space. We parameterize it by Euler angles (θ, φ, ψ):

$$\mathbf{Q} = \begin{pmatrix} \cos\varphi\cos\psi - \cos\theta\sin\psi\sin\varphi & \cos\varphi\sin\psi + \cos\theta\cos\psi\sin\varphi & \sin\varphi\sin\theta \\ -\sin\varphi\cos\psi - \cos\theta\sin\psi\cos\varphi & -\sin\varphi\sin\psi + \cos\theta\cos\psi\cos\varphi & \cos\varphi\sin\theta \\ \sin\theta\sin\psi & -\sin\theta\cos\psi & \cos\theta \end{pmatrix}$$

As coordinates in the tangent space $T_x\mathcal{N}$ we choose the projections of the angular velocity of the body, $\boldsymbol{\omega} = (\omega_1, \omega_2, \omega_3)$, onto the axes of the moving coordinate system:

$$\omega_1 = \dot{\psi}\sin\theta\sin\varphi + \dot{\theta}\cos\varphi, \quad \omega_2 = \dot{\psi}\sin\theta\cos\varphi - \dot{\theta}\sin\varphi, \quad \omega_3 = \dot{\psi}\cos\theta + \dot{\varphi}. \tag{2}$$

In the coordinate system $Ox_1x_2x_3$ we obtain $\boldsymbol{e} = (0, 0, 1)$, and hence the constraint equation (1) has the form

$$\omega_3 = 0. \tag{3}$$

Regarding the mass distribution of the rigid body and the positions of the rotors we make additional assumptions:

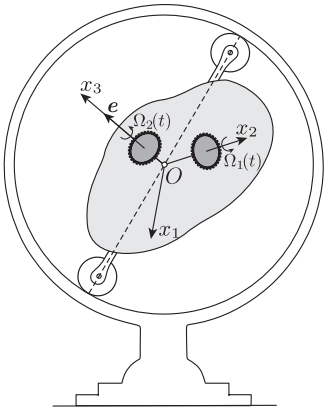

Figure 1. Realization of the Suslov problem.

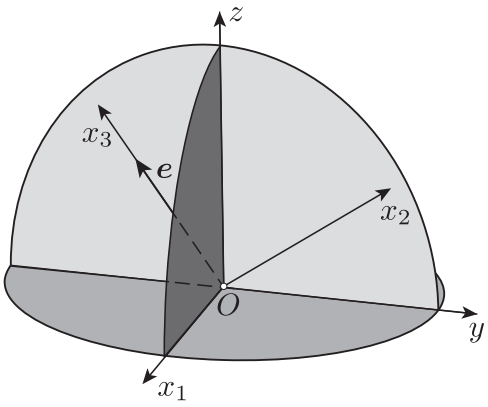

Figure 2. Positions of the axes of the moving coordinate system $Ox_1x_2x_3$ and the principal planes of inertia in the cases $I_{12} = 0$ and $I_{13} = 0$, here Ox_1yz are the principal axes of inertia of the system.

(a) The vector **e**, which defines the constraint (1), is perpendicular to one of the principal axes of inertia of the system, which we take to be the axis Ox_1 (see figure 2), so that the tensor of inertia (rigid body + rotors) takes the form

$$\mathbf{I} = \begin{pmatrix} I_{11} & 0 & 0 \\ 0 & I_{22} & I_{23} \\ 0 & I_{23} & I_{33} \end{pmatrix}$$

(b) The axis of rotation of the first and the second rotor coincides, respectively, with the coordinate axes $\mathrm{O}x_2$ and $\mathrm{O}x_3$.

The kinetic energy of the entire system can be represented as

$$T = \frac{1}{2}\,(\boldsymbol{\omega}, \mathbf{I}\boldsymbol{\omega}) + (\boldsymbol{\omega}, \boldsymbol{k}(t))\,,$$

where $\boldsymbol{k}(t)$ is the gyrostatic momentum of the system, which is expressed in terms of the moments of inertia J_1, J_2 and the angular velocities of the rotors $\Omega_1(t)$, $\Omega_2(t)$ by the formula

$$\boldsymbol{k}(t) = (0,\, J_1\Omega_1(t),\, J_2\Omega_2(t))\,.$$

The equations of motion for $\boldsymbol{\omega}$ in the moving coordinate system $Ox_1x_2x_3$ are

$$\frac{\mathrm{d}}{\mathrm{d}t}\left(\frac{\partial T}{\partial \boldsymbol{\omega}}\right) = \frac{\partial T}{\partial \boldsymbol{\omega}} \times \boldsymbol{\omega} + N\boldsymbol{e}, \tag{4}$$

where N is the undetermined multiplier, which is the torque of the constraint reaction.

As can be seen, the multiplier N appears in this case only in the last equation of the system (4). From this equation, taking the constraint (3) into account, one can express N as a function of angular velocities and time. As a result, the equations of motion for the angular velocities ω_1 and ω_2 decouple and can be represented as

$$I_{11}\dot{\omega}_1 = -\left(I_{23}\omega_2 + k_3(t)\right)\omega_2, \quad I_{22}\dot{\omega}_2 = \left(I_{23}\omega_2 + k_3(t)\right)\omega_1 - \dot{k}_2(t). \tag{5}$$

From a known solution of this system $\boldsymbol{\omega}(t) = (\omega_1(t),\, \omega_2(t), 0)$, according to (2), the orientation of the body is described by the following system of equations for the Euler angles

$$\dot{\theta} = \omega_1 \cos\varphi - \omega_2 \sin\varphi, \quad \dot{\varphi} = -\frac{\cos\theta}{\sin\theta}\left(\omega_1 \sin\varphi + \omega_2 \cos\varphi\right),$$
$$\dot{\psi} = \frac{\omega_1 \sin\varphi + \omega_2 \cos\varphi}{\sin\theta}.$$

When it comes to finding various dynamical regimes in the system under study, it is of interest to consider the case $I_{23} \neq 0$. Introducing new variables and functions

$$v = -\frac{I_{23}}{I_{22}}\omega_1, \quad u = \frac{I_{23}}{\sqrt{I_{11}I_{22}}}\omega_2,$$
$$K(t) = \frac{k_3(t)}{\sqrt{I_{11}I_{22}}}, \quad \Lambda(t) = \frac{I_{23}k_2(t)}{I_{22}\sqrt{I_{11}I_{22}}} \tag{6}$$

yields a reduced system which will be the subject of our study in what follows:

$$\dot{u} = -vu - K(t)v - \dot{\Lambda}(t), \quad \dot{v} = u^2 + K(t)u. \tag{7}$$

Of particular interest is the question of whether trajectories unbounded on the plane (v, u) exist (depending on the choice of functions $K(t)$ and $\Lambda(t)$) (i.e., the possibility of unbounded speedup), as well as the question of the existence of regular and chaotic regimes of motion in this system.

Remark 1. After the transformation (6), the dependence on the moments of inertia of the rigid body and on gyrostatic momentum in the reduced system (7) can be defined by two functions $K(t)$ and $\Lambda(t)$.

Next, we assume the functions $K(t)$ and $\Lambda(t)$ to be periodic with the same period T. In this case, taking the equation $\dot{t} = 1$ into account, one can assume that the system (7) describes the vector field on the manifold

$$\mathcal{M}^3 = \{(u, v, t \bmod T)\} \approx \mathbb{R}^2 \times S^1.$$

Remark 2. One can also consider the case where excitation is given by a quasi-periodic function. In this case, one can assume $K(\theta_1, \theta_2)$, $\Lambda(\theta_1, \theta_2)$, where

$$\dot{\theta}_1 = \Omega_1, \quad \dot{\theta}_2 = \Omega_2,\ \Omega_1, \Omega_2 = \text{const},$$

in particular, for $K(\theta_1)$ and $\Lambda(\theta_2)$ we obtain periodic functions with different periods. In this case, the flow of the system (7) turns out to be defined on the four-dimensional manifold

$$\mathcal{M}^4 = \{(u, v, \theta_1 \bmod T_1, \theta_2 \bmod T_2)\} \approx \mathbb{R}^2 \times S^1 \times S^1,$$

and its analysis requires construction of a three-dimensional Poincaré map.

The undetermined multiplier that defines the torque of the constraint reaction can be represented in the chosen variables as

$$N = \frac{\sqrt{I_{11}I_{22}}}{I_{23}^2}\left((I_{11}I_{22} - I_{22}^2 - I_{23}^2)uv - \left(I_{22}^2\Lambda(t) + I_{23}^2K(t)\right)v + I_{23}^2\left(\dot{K}(t) - \dot{\Lambda}(t)\right)\right). \quad (8)$$

Remark 3. If $I_{23} = 0$, then the system (5) reduces to a linear system and possesses linear integrals explicitly depending on time:

$$F_1 = I_{11}\sqrt{I_{22}}\omega_1 \cos\kappa(t) + I_{22}\sqrt{I_{11}}\omega_2 \sin\kappa(t) + \int I_{11}\dot{k}_2 \sin\kappa(t)\,\mathrm{d}t,$$

$$F_2 = I_{11}\sqrt{I_{22}}\omega_1 \sin\kappa(t) - I_{22}\sqrt{I_{11}}\omega_2 \cos\kappa(t) - \int I_{11}\dot{k}_2 \cos\kappa(t)\,\mathrm{d}t,$$

$$\kappa(t) = \frac{\int k_3(t)\,\mathrm{d}t}{\sqrt{J_{11}J_{22}}}.$$

Thus, on the fixed level set of the integrals $F_1 = f_1$ and $F_2 = f_2$, the angular velocities ω_1 and ω_2 are given by explicit quadratures.

2. An additional integral and quantization of the rotation number

Let $\Lambda = \text{const}$ (for example, if the gyrostatic momentum is directed along the vector $\boldsymbol{e}$, we obtain $\Lambda = 0$). Then the system (7) can be represented as

$$\dot{u} = -v\,(u + K(t)), \quad \dot{v} = u\,(u + K(t)) \quad (9)$$

and possesses an additional integral

$$F(\boldsymbol{x}) = v^2 + u^2. \quad (10)$$

The fixed level set of this integral $F(\boldsymbol{x}) = \text{const}$ on the plane $\mathbb{R}^2 = \{(u, v)\}$ defines a circle, therefore, the functions $u(t)$ and $v(t)$ are bounded and *hence an unbounded speedup of the body is impossible*.

On the fixed level set of the integral $F(\boldsymbol{x}) = f^2$, we introduce the angular coordinate

$$v = f \sin\Phi, \quad u = f \cos\Phi.$$

The equation governing the evolution of the angle Φ can be represented as

$$\dot{\Phi} = f \cos\Phi + K(t). \quad (11)$$

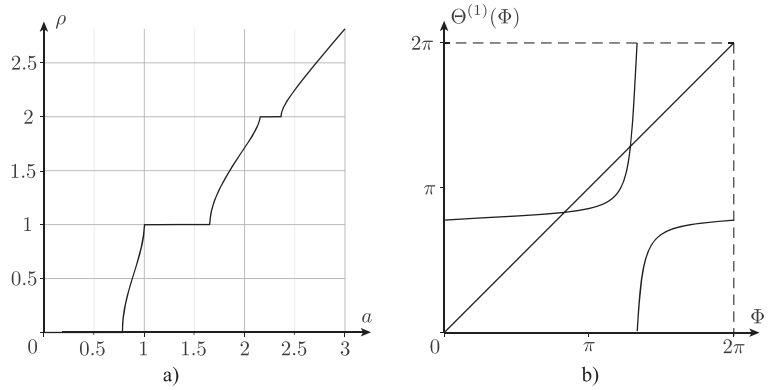

Figure 3. (a) Graph showing the dependence of the rotation number ρ on a, constructed numerically for $K(t) = a + b\sin(t)$ with fixed $f = 1$, $b = 1$. (b) The first iteration of the map $\Theta(\Phi)$ and the diagonal of the square for the values $a = 1.5$.

$K(t)$ is assumed to be a periodic function of time. Therefore, if we add to equation (11)

$$\dot{t} = 1, \tag{12}$$

then we obtain a vector field on the torus $\mathbb{T}^2 = \{(\Phi \bmod 2\pi,\ t \bmod T)\}$ (without fixed points). In this case there exists an invariant, *the rotation number*, which for the system (11) can be calculated by the formula

$$\rho = \frac{T}{2\pi}\lim_{t\to\infty}\frac{\Phi(t)}{t}.$$

As is well known, in the general case, for systems (11) and (12) without a continuous invariant measure, the graph showing the dependence of the rotation number on the system parameters is a Cantor ladder: corresponding to each rational value of the rotation number ρ there is a horizontal segment which corresponds to a torus with one or several limit cycles [32].

In [33–35] it is shown that no Cantor ladder arises for systems of the form (11), and the graph of the rotation number depending on a parameter is a set of horizontal segments with integer rotation numbers ($\rho = n,\ n \in \mathbb{Z}$), which are connected by smooth curves (see figure 3(a)). Corresponding to horizontal segments is also one or several limit cycles on the torus $\mathbb{T}^2$. If ρ does not take an integer value, then all trajectories on the torus $\mathbb{T}^2$ are either periodic ($\rho \in \mathbb{Q}$) or quasi-periodic ($\rho \notin \mathbb{Q}$). The above-mentioned property is due to the fact that the general solution (11) is expressed in terms of solutions to the linear system with periodic coefficients [33].

Thus, the trajectories of the system (11) and hence (9) can be only of the following types (see [33] for details):

(a) *All trajectories are quasi-periodic or periodic*;
(b) *There are several limit cycles and all trajectories tend from an unstable limit cycle to a stable one*.

To find the corresponding limit cycles, one can use the Poincaré map of the system on the torus (11). Choosing as a secant the circle $t = 0$ (which is intersected by all trajectories due to

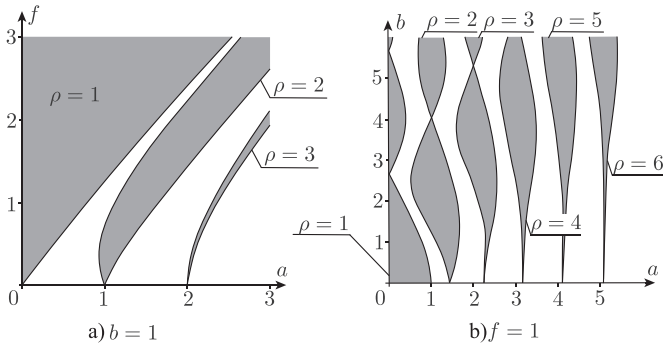

Figure 4. The region on the parameter plane for $K(t) = a + b\sin(t)$ in which the rotation number ρ takes an integer value (gray).

the equation (12)), we obtain a map of the circle onto itself:

$$\Theta(\Phi) : S^1 \to S^1.$$

Figure 3(b) shows a graph of the first iteration of this map. The curve $\Theta^{(1)}(\Phi)$ is seen to intersect the diagonal (of the square), and their intersection points correspond to the periodic solutions of (11), for example, in figure 3(b) one can see two limit cycles.

Regions with an integer value of the rotation number ρ (Arnol'd tongues) on the parameter plane of the system are depicted in figure 4. Thus, for the parameters of the system (11) and (12) for which ρ takes an integer value, the trajectory of this system asymptotically tends to a limit cycle in which the angular velocity of the body periodically changes with time. A detailed discussion of the structure of these regions for systems of the form (11) can be found in [36].

3. Dynamics for large v and nonlinear speedup

The case $K(t) = 0$. In this case, the reduced system (7) coincides with a reduced system describing a different nonholonomic system—*the Chaplygin sleigh with gyrostatic momentum*. The following result [23] holds for this system.

Theorem 1. *Let $\Lambda(t)$ be a periodic function. Let us calculate the following average value:*

$$\langle\dot\Lambda^2\rangle = \frac{1}{T}\int_0^T \dot\Lambda^2(t)\mathrm{d}t.$$

If $v(0) > 0$ at the initial time instant, then, as $t \to +\infty$, the function $v(t)$ increases indefinitely and $u(t)$ tends to zero:

$$v(t) = Ct^{\frac{1}{3}} + o\left(t^{\frac{1}{3}}\right), \quad u(t) = -C\dot\Lambda(t)t^{-\frac{1}{3}} + o\left(t^{-\frac{1}{3}}\right), \quad C = \left(3\langle\dot\Lambda^2\rangle\right)^{\frac{1}{3}}.$$

In addition, it is shown in [23] that in this case the sleigh has mean motion in some fixed direction, and the constraint reaction is a bounded function of time. Thus, the Chaplygin sleigh can be accelerated without violating the nonholonomic constraint. In the Suslov system (4) the situation is much different: as is seen from (8), the constraint reaction contains terms

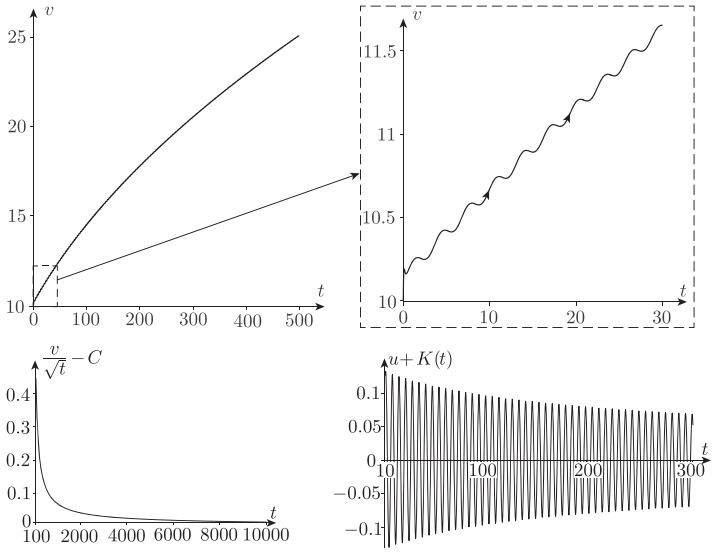

Figure 5. Dependences obtained numerically for $\Lambda(t) = \sin t$, $K(t) = \cos t$ ($\langle G \rangle > 0$) and the initial conditions $u(0) = 2$, $v(0) = 10$.

linear in v and is not a bounded function during speedup. Evidently, this will lead to a violation of the constraint (1) at large v and to lateral slipping at the points of contact of the wheels (see figure 1) (but in this paper we do not analyze this problem).

The case $K(t) \neq 0$. In what follows, using some assumptions, we obtain a condition for the functions $K(t)$ and $\Lambda(t)$ under which the system (7) has unbounded trajectories.

Let $|u| \gg 1$, $v \gg 1$ at the initial time instant. Then the quadratic terms become leading in the system (7). We recall (see, e.g. [9]), that they describe a vector field whose trajectories are attracted to the positive axis

$$\mathbb{R}_+ = \{v \gg 1, u = 0\},$$

and preserve the integral (10). Thus, v remains a fairly large quantity, and for u the inequality $|u| \gg 1$ is violated in the course of time.

Numerical experiments show that in the region $\mathbb{R}_+$ the variable $v(t)$ changes weakly as compared to $u(t)$ (see figures 6 and 9). Therefore, we integrate the first equation of (7), assuming that v takes a constant value:

$$u(t) = C\mathrm{e}^{-vt} - \mathrm{e}^{-vt} \int \mathrm{e}^{vt} \left(vK(t) + \dot{\Lambda}(t) \right) \mathrm{d}t.$$

Integrating this relation by parts, using the condition $v \gg 1$ and neglecting terms of order v^{-3} and higher, we obtain

$$u(t) = -K(t) + \frac{\dot{K}(t) - \dot{\Lambda}(t)}{v} + \frac{\ddot{\Lambda}(t)}{v^2} + \dots.$$

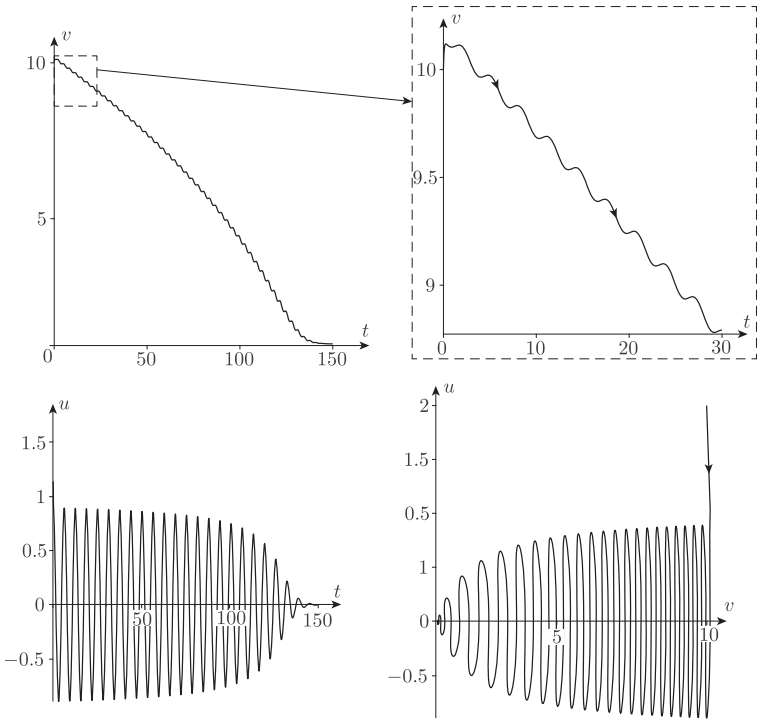

Figure 6. Dependences obtained numerically for $\Lambda(t) = \sin t$, $K(t) = -\cos t$ ($\langle G\rangle < 0$) and the initial conditions $u(0) = 2$, $v(0) = 10$.

Substituting the resulting relation into the second equation of (7) and neglecting terms v^{-2} and higher, we find

$$\dot v = \frac{K(t)\left(\dot\Lambda(t) - \dot K(t)\right)}{v} + \cdots .$$

From the relation thus obtained we see that, if one neglects higher-order terms, then

$$\left(v^2\right)^{\cdot} = G(t) = 2K(t)\left(\dot\Lambda(t) - \dot K(t)\right),$$

where $G(t) = G(t+T)$. As is well known, in this case the evolution of $v^2(t)$ is given by the relation

$$v^2 = \langle G\rangle t + H(t), \quad H(t) = H(t+T).$$

Noting that $\langle K\dot K\rangle = \langle \left(\frac{1}{2}K^2\right)^{\cdot}\rangle = 0$, we obtain the following conjecture.

Conjecture of acceleration. If the average

$$\langle G\rangle = \frac{1}{T}\int_0^T 2K(t)\dot\Lambda(t)\mathrm{d}t > 0, \tag{13}$$

then the system (7) has trajectories unbounded in v, which have the following asymptotics:

$$v(t) = Ct^{\frac{1}{2}} + o\left(t^{\frac{1}{2}}\right), \quad u(t) = -K(t) + o\left(t^{-\frac{1}{2}}\right), \quad C = \sqrt{\langle G\rangle}. \tag{14}$$

If $\langle G\rangle < 0$, then there are no unbounded trajectories. The case $\langle G\rangle = 0$ requires a separate analysis.

As can be seen, in the above cases of acceleration, ($K(t) = 0$), and existence of an additional integral, ($\Lambda(t) = 0$), we have $\langle G\rangle = 0$. In addition, condition (13) and asymptotics (14) are in good agreement with numerical calculations (see figure 5) for the initial conditions $u, v \gg 1$. If $\langle G\rangle < 0$, then numerical experiments (see figure 6) show that for $u, v \gg 1$ the velocity decreases (i.e., the body slows down) and the trajectory leaves the region $u, v \gg 1$. In this case, the system can exhibit a strange attractor (see the next section).

Remark 4. We note that the proof of the theorem as presented in [23] is based on the fact that the function $v(t)$ in (7) is monotonic for $K(t) = 0$. As can be seen (e.g., from figure 5), this does not hold true in the general case, and it is impossible to generalize this proof.

4. Coexistence of a strange attractor and unbounded trajectories (speedup)

As noted above, in the Chaplygin sleigh problem [23], in the presence of acceleration, all trajectories of the reduced system are unbounded. We show that in this case one can choose the functions $\Lambda(t)$ and $K(t)$ in such a way that, with acceleration present in the system, it can have a strange attractor.

As an example, we choose a one-parameter family of functions

$$\Lambda(t) = \frac{\sin t}{2} - \alpha \cos t, \quad K(t) = \sin t, \quad \alpha = \text{const}.$$

In this case, the reduced system of equation (7) can be represented as

$$\dot{u} = -v\,u - v \sin t - \alpha \sin t - \frac{\cos t}{2}, \quad \dot{v} = u^2 + u \sin t. \tag{15}$$

Since the right-hand side depends periodically on time, the vector field (15) generates a period advance map of the plane (a Poincaré map), which we investigate numerically.

In this case, the quantity (13), which defines the average evolution of v^2, has the form

$$\langle G\rangle = \frac{\alpha}{2}.$$

By the hypothesis of acceleration, it is necessary to consider two situations, according as whether the system (15) has unbounded trajectories ($\alpha > 0$) or has none ($\alpha \leqslant 0$).

The case $\alpha \leqslant 0$. Then all trajectories of the system (15) are bounded. Numerical experiments show that in this case one can observe the following two qualitatively different dynamical regimes.

(a) *Stability and multistability*: as $t \to +\infty$, all trajectories tend to one or several periodic solutions of the system (15) (see figure 7).

(b) *Chaotic oscillations*: the system exhibits a strange attractor (see figure 8) which attracts all trajectories of the system. In particular, this also holds for $\alpha = 0$. A typical view of a Poincaré map is shown in figure 9.

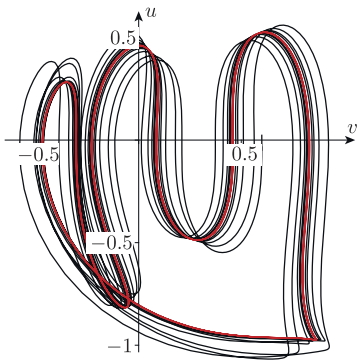

Figure 7. A Poincaré map and the dependence $u(v)$ for the fixed parameter $\alpha = -0.2$ and the initial conditions $t = 0$, $v = 0.6$, $u = 0.06$. Red denotes a limit cycle. In this case, a cycle of period 3 (consisting of isolated points) arises on the Poincaré map.

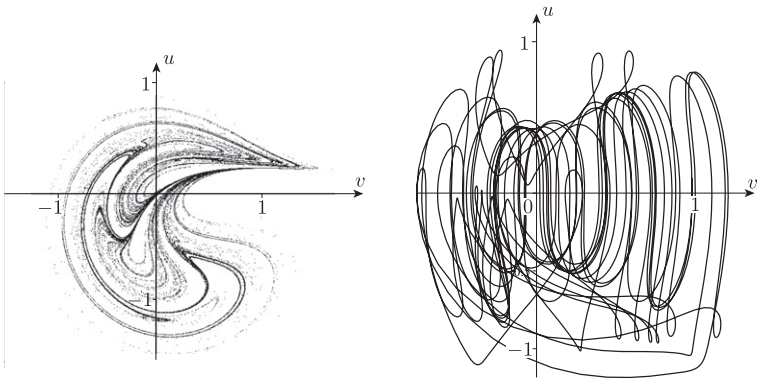

Figure 8. A Poincaré map and the dependence $u(v)$ for the fixed parameter $\alpha = -0.05$ and the initial conditions $t = 0$, $v = 1$, $u = 1$.

For a chaotic trajectory corresponding to a strange attractor for the parameters in figure 8, the Lyapunov exponents are[5]

$$\lambda_1 \approx 0.087, \quad \lambda_2 \approx -0.262, \quad \lambda_3 \approx 0$$

The dimension of this attractor on the map, estimated from the Kaplan – Yorke formula [38], is

$$D = 1 + \frac{\lambda_1}{|\lambda_2|} \approx 1.33.$$

The case $\alpha > 0$. Depending on the value of the parameter α, the system (15) has the following regimes.

(a) *Chaotic oscillations and speedup*: there are unbounded and bounded trajectories, which are attracted to a strange attractor.

[5] One zero value of the Lyapunov exponent corresponds to a shift in the trajectory [37].

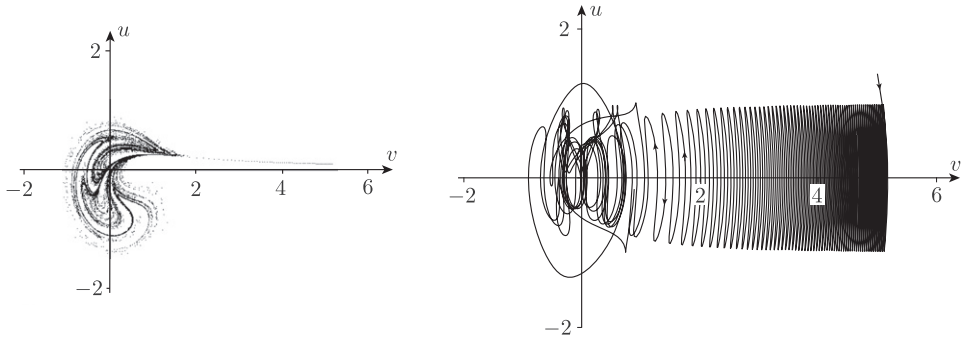

Figure 9. A Poincaré map and the dependence $u(v)$ for the fixed parameter $\alpha = 0$ and the initial conditions $t = 0$, $v = 5$, $u = 1.4$.

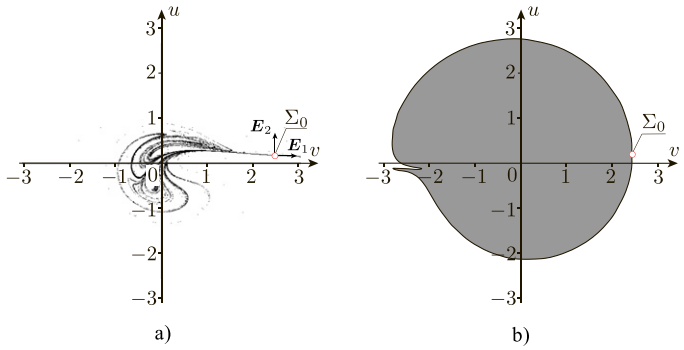

Figure 10. The fixed parameter $\alpha = 0.1$ (a) a Poincaré map and (b) location of the domain of attraction of the attractor (gray) and of the fixed point of the map Σ_0.

(b) *Speedup*: except for the unstable fixed points of the map, all trajectories are noncompact; in this case, $v \to +\infty$ as $t \to +\infty$. Numerical experiments show that their asymptotics is described by (14).

If $\alpha > 0$, but is smaller than some critical value α_*, then the map exhibits both noncompact and bounded chaotic trajectories (see figure 10(a)). In this case, the map has an unstable fixed point Σ_0.

Figure 10(b) shows a numerically constructed basin of attraction of a strange attractor. The fixed point of the map Σ_0 lies in the boundary of this basin of attraction and corresponds to a periodic solution of the system (15). The multipliers of the periodic solution Σ_0 are, to within the error of calculation, equal to

$$\Lambda_1 \approx 1.047 \pm 10^{-3}, \quad \Lambda_2 \approx 0.0 + 10^{-6}$$

over the whole range $0 < \alpha < \alpha_0^*$. A weak expansion can be observed in the direction of the eigenvector $\boldsymbol{E}_1$, whereas in the direction $\boldsymbol{E}_2$ a strong compression arises, so that the fixed point on the map is degenerate (to within the error of calculation). Thus, the basin of attraction of the strange attractor is bounded by the stable invariant manifold (incoming separatrix) Γ_s of point Σ_0. A similar situation arises in the two-dimensional Hénon map [39]. At the same

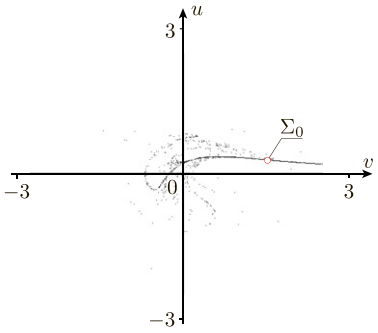

Figure 11. A Poincaré map for the fixed parameter $\alpha = 0.15$ and for different initial conditions.

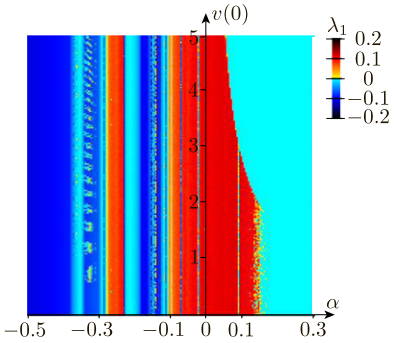

Figure 12. Chart of the largest Lyapunov exponent λ_1 for a trajectory with the fixed initial conditions $t = 0$ and $u = 0$, but with different values of the parameter α and different initial conditions for the variable v.

time, the smallness of the eigenvalue of Λ_2 makes it extremely difficult to numerically obtain the separatrix Γ_s.

As α increases, the point Σ_0 approaches the origin of coordinates. Numerical experiments show that, after reaching the critical value $\alpha = \alpha_*$, all trajectories, except for the above-mentioned fixed point Σ_0 and the unstable fixed points of the map, become unbounded (see figure 11).

The situation described above is clearly illustrated by the chart of the largest Lyapunov exponent λ_1, which is shown in figure 12. In the region $\alpha < 0$, the trajectory tends, regardless of $v(0)$, to a limit cycle ($\lambda_1 < 0$) or to a strange attractor ($\lambda_1 > 0$). In the region $\alpha > 0$, as α increases depending on $v(0)$, there are regions in which a strange attractor ($\lambda_1 > 0$) and unbounded trajectories ($\lambda_1 < 0$) are observed. Then, after the critical value of α has been reached, only unbounded trajectories are observed.

5. Reversibility and coexistence of a strange attractor and a strange repeller

If $\alpha = 0$, then the system (15) has the involution

$$u \to -u, \quad v \to -v, \quad t \to -t, \tag{16}$$

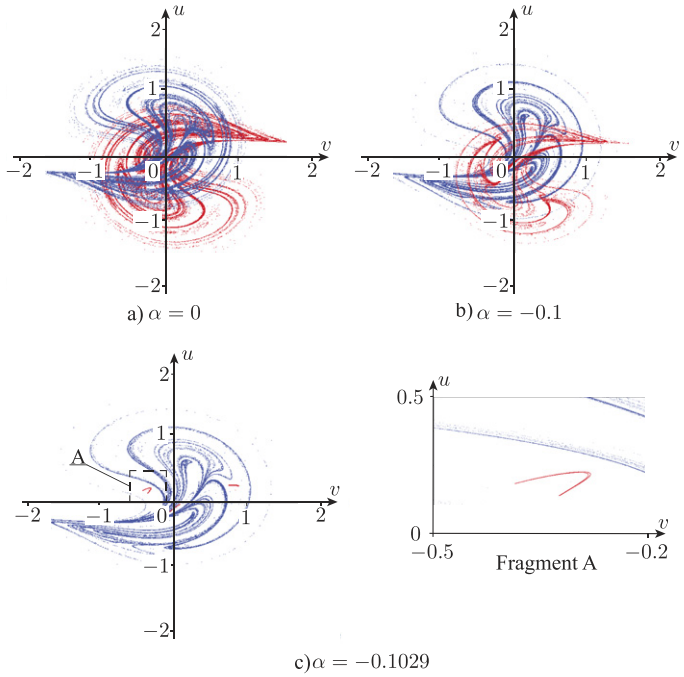

Figure 13. A Poincaré map in forward (red) and backward (blue) time for different values of the parameter α and the fixed initial conditions $t = 0$, $u = 1$, $v = 1$.

i.e., the system turns out to be reversible. As is well known, in this case the attractors and repellers occur as pairs and are symmetric with respect to the involution (16). For example, a strange attractor and a strange repeller arise simultaneously, see figure 13(a). When $\alpha \neq 0$, the involution (16) is absent; as a result, the attractor and the repeller become asymmetric with respect to the involution (16) (figures 13(b) and (c)).

In figure 13(c), the strange attractor coexists with the strange repeller. As the parameter α increases, the strange attractor 'merges' with the strange repeller [40, 41], giving rise to mixed dynamics. Interestingly, this system exhibits a new type of mixed dynamics in which the closure of the strange attractor intersects with that of the strange repeller in an irreversible system (13b). Earlier, this phenomenon was observed in the model of coupled oscillators [42]. In nonholonomic mechanics, mixed dynamics in an irreversible system has been discovered for the first time. We note that the phenomenon of intersection of the closure of a strange attractor and a repeller (mixed dynamics) is discussed in detail in [43].

As α decreases further, the trajectories for $t \to +\infty$ asymptotically tend to a limit cycle or a strange attractor, and those for $t \to -\infty$ are unbounded (that is, the system becomes in fact dissipative). Many dynamical systems arising in nonholonomic mechanics are reversible [44, 45]. However, as we have seen in the above example, this is not always the case.

In this and the previous sections, the chart of Lyapunov exponents and the Poincaré map have been constructed using the software package computer dynamics: Chaos (see http://site4.ics.org.ru/chaos_pack/), which was developed at the Institute of Computer Science of the Udmurt State University. The system of differential equations of motion is solved numerically by the Runge–Kutta–Werner method of the sixth order of accuracy with control of the integration error.

Acknowledgments

The authors express their gratitude to A V Borisov and A O Kazakov for fruitful discussions and useful comments. The work of I A Bizyaev was supported by the RFBR Grant No. 18-31-00344 mol_a and was supported from a grant to the Ural Mathematical Center in the framework of the national project 'Science' of the Russian Federation. The work of I S Mamaev was carried out within the framework of the state assignment or the Ministry of Education and Science of Russia (FZZN-2020-0011).

ORCID iDs

Ivan S Mamaev https://orcid.org/0000-0003-3916-9367

References

[1] Fernandez O E, Bloch A M and Zenkov D V 2014 The geometry and integrability of the Suslov problem *J. Math. Phys.* **55** 112704
[2] Fernandez O E and Bloch A M 2008 Equivalence of the dynamics of nonholonomic and variational nonholonomic systems for certain initial data *J. Phys. A: Math. Theor.* **41** 344005
[3] Garcia-Naranjo L C 2019 Generalisation of Chaplygin's reducing multiplier theorem with an application to multi-dimensional nonholonomic dynamics *J. Phys. A: Math. Theor.* **52** 205203
[4] Borisov A V, Kilin A A and Mamaev I S 2012 How to control Chaplygin's sphere using Rotors *Regul. Chaotic Dyn.* **17** 258–72
[5] Kilin A A, Pivovarova E N and Ivanova T B 2015 Spherical robot of combined type: dynamics and control *Regul. Chaotic Dyn.* **20** 716–28
[6] Lynch P and Bustamante M D 2009 Precession and recession of the rock'n'roller *J. Phys. A: Math. Theor.* **42** 425203
[7] Suslov G K 1946 *Theoretical Mechanics* (Moscow: Gostekhizdat)
[8] Vagner V V 1941 A geometric interpretation of nonholonomic dynamical systems *Tr. semin. po vectorn. i tenzorn. anal.* **5** 301–27
[9] Borisov A V, Kilin A A and Mamaev I S 2011 Hamiltonicity and integrability of the Suslov problem *Regul. Chaotic Dyn.* **16** 104–16
[10] Kozlov V V 2002 On the integration theory of equations of nonholonomic mechanics *Regul. Chaotic Dyn.* **7** 191–76
[11] Fedorov Yu N, Maciejewski A J and Przybylska M 2009 Suslov problem: integrability, meromorphic and hypergeometric solutions *Nonlinearity* **22** 2231–59
[12] Bizyaev I A, Bolsinov A V, Borisov A V and Mamaev I S 2015 Topology and bifurcations in nonholonomic mechanics *Int. J. Bifurcation Chaos Appl. Sci. Eng.* **25** 1530028
[13] Kharlamov A P and Kharlamov M P 1995 A nonholonomic Hinge *Mekh. Tverd. Tela* **27** 1–7
[14] Bizyaev I A, Borisov A V and Mamaev I S 2014 The dynamics of nonholonomic systems consisting of a spherical shell with a moving rigid body inside *Regul. Chaotic Dyn.* **19** 198–213
[15] Bizyaev I A, Borisov A V and Kazakov A O 2015 Dynamics of the Suslov problem in a gravitational field: reversal and strange attractors *Regul. Chaotic Dyn.* **20** 605–26
[16] Kharlamova-Zabelina E I 1957 Rapid rotation of a rigid body around a fixed point in the presence of a nonholonomic constraint *Vestn. Mosk. Univ. Ser. 1. Mat. Mekh.* **6** 25–34
[17] Garcia-Naranjo L C, Maciejewski A J, Marrero J C and Przybylska M 2014 The inhomogeneous Suslov problem *Phys. Lett.* A **378** 2389–94
[18] Jovanovic B 1998 Non-holonomic geodesic flows on Lie groups and the integrable Suslov problem on $SO(4)$ *J. Phys. A: Math. Gen.* **31** 1415
[19] Zenkov D V and Bloch A 2000 M Dynamics of the n-dimensional Suslov problem *J. Geom. Phys.* **34** 121–36
[20] Maciejewski A J and Przybylska M 2002 Non-integrability of the Suslov problem *Regul. Chaotic Dyn.* **7** 73–80

[21] Maciejewski A J and Przybylska M 2004 Nonintegrability of the Suslov problem *J. Math. Phys.* **45** 1065–78
[22] Bizyaev I A, Borisov A V and Mamaev I S 2017 The Chaplygin Sleigh with parametric excitation: Chaotic dynamics and nonholonomic acceleration *Regul. Chaotic Dyn.* **22** 955–75
[23] Bizyaev I A, Borisov A V, Kozlov V V and Mamaev I S 2019 Fermi-like acceleration and power-law energy growth in nonholonomic systems *Nonlinearity* **32** 3209–33
[24] Bizyaev I A, Borisov A V and Kuznetsov S P 2017 Chaplygin sleigh with periodically oscillating internal mass *Europhys. Lett.* **119** 60008
[25] Kilin A A and Pivovarova E N 2018 Chaplygin top with a periodic gyrostatic moment *Russ. J. Math. Phys.* **25** 509–24
[26] Kozlov V 2016 The phenomenon of reversal in the Euler – Poincare – Suslov nonholonomic systems *J. Dyn. Contr. Syst.* **22** 713–24
[27] Fedorov Y N and Garcia-Naranjo L C 2010 The hydrodynamic Chaplygin sleigh *J. Phys. A: Math. Theor.* **43** 434013
[28] Bizyaev I A, Borisov A V and Kuznetsov S P 2019 The Chaplygin sleigh with friction moving due to periodic oscillations of an internal mass *Nonlinear Dynam.* **95** 699–714
[29] Fedonyuk V and Tallapragada P 2018 Sinusoidal control and limit cycle analysis of the dissipative Chaplygin sleigh *Nonlinear Dynam.* **93** 835–46
[30] Armour R H and Vincent J F V 2006 Rolling in nature and robotics: a review *Journal of Bionic Engineering* **3** 195–208
[31] Nagarajan U, Kantor G and Hollis R L 2009 Trajectory planning and control of an underactuated dynamically stable single spherical wheeled mobile robot *2009 IEEE International Conference on Robotics and Automation* pp 3743–8
[32] Arnold V I 1961 Small denominators: 1 mapping the Circle onto itself *Izv. Akad. Nauk SSSR Ser. Mat.* **1** 21–86
[33] Bizyaev I A, Borisov A V and Mamaev I S 2017 The Hess – Appelrot case and quantization of the rotation number *Regul. Chaotic Dyn.* **22** 180–96
[34] Buchstaber V M, Karpov O V and Tertychniy S I 2010 Rotation number quantization effect *Theor. Math. Phys.* **162** 211–21
[35] Ilyashenko Y S, Ryzhov D A and Filimonov D A 2011 Phase-lock effect for equations modeling resistively shunted Josephson junctions and for their perturbations *Funct. Anal. Appl.* **45** 192–203
[36] Buchstaber V M and Glutsyuk A A 2017 On monodromy eigenfunctions of Heun equations and boundaries of phase-lock areas in a model of overdamped Josephson effect *Proc. Steklov Inst. Math.* **297** 50–89
[37] Sprott J C 2010 *Elegant Chaos: Algebraically Simple Chaotic Flows* (Singapore: World Scientific)
[38] Kaplan J L and Yorke J A 1979 A Chaotic behavior of multi-dimensional differential equations *Functional Differential Equations and Approximations of Fixed Points* Lecture Notes in Mathematics vol 730 H O Peitgen and H O Walther (Berlin: Springer) pp 204–27
[39] Simo C 1979 On the Henon-Pomeau attractor *J. Stat. Phys.* **21** 465–94
[40] Gonchenko A S, Gonchenko S V, Kazakov A O and Turaev D V 2017 On the phenomenon of mixed dynamics in Pikovsky – Topaj system of coupled rotators *Physica* D **350** 45–57
[41] Kazakov A O 2019 On the appearance of mixed dynamics as a result of collision of strange attractors and repellers in reversible systems *Radiophys. Quantum Electron.* **61** 650–8
[42] Emelianova A A and Nekorkin V I 2019 On the intersection of a chaotic attractor and a chaotic repeller in the system of two adaptively coupled phase oscillators *Chaos* **29** 111102
[43] Gonchenko S V and Turaev D V 2017 On three types of dynamics and the notion of attractor *Proc. Steklov Inst. Math.* **297** 116–37
[44] Borisov A V, Mamaev I S and Bizyaev I A 2013 The hierarchy of dynamics of a rigid body rolling without slipping and spinning on a plane and a sphere *Regul. Chaotic Dyn.* **18** 277–328
[45] Borisov A V, Kazakov A O and Sataev I R 2014 The reversal and chaotic attractor in the nonholonomic model of Chaplygins top *Regul. Chaotic Dyn.* **19** 718–33